Tracing the Efficient Curve for Multi-Objective Control-Structure Optimization

By Joanna Rakowska, Raphael T. Haftka, and Layne T. Watson

TR 91-2

TRACING THE EFFICIENT CURVE FOR MULTI-OBJECTIVE CONTROL-STRUCTURE OPTIMIZATION

JOANNA RAKOWSKA[†], RAPHAEL T. HAFTKA[‡], AND LAYNE T. WATSON[+]

Abstract. A recently developed active set algorithm for tracing parametrized optima is adapted to multi-objective optimization. The algorithm traces a path of Kuhn-Tucker points using homotopy curve tracking techniques, and is based on identifying and maintaining the set of active constraints. Second order necessary optimality conditions are used to determine nonoptimal stationary points on the path. In the bi-objective optimization case the algorithm is used to trace the curve of efficient solutions (Pareto optima). As an example, the algorithm is applied to the simultaneous minimization of the weight and control force of a ten-bar truss with two collocated sensors and actuators, with some interesting results.

1. Introduction. In recent years there has been considerable interest in simultaneous control-structure optimization of space structures [4]. Although the problem can be solved by sequential optimization of a structure objective (J_s) and a control system objective (J_c), better designs are obtained when both objectives are optimized simultaneously (e.g., [5]). In the latter approach both objectives are combined into a bi-objective cost function $\mathcal{J} = (J_s, J_c)$. Bi-objective optimization gives the designs (known as *efficient* solutions) where one objective can be improved only at the expense of the other one. Such a formulation of the problem produces a family of design options which can be used in the early stages of the design process to guide the evolution of the design [2].

The optimal solutions to the problem of minimizing the bi-objective cost function $\mathcal{J} = (J_s, J_c)$ can be found by optimizing the convex combination $(1-\alpha)J_s + \alpha J_c$ of J_s and J_c [2]. Homotopy curve tracking methods can be used to generate the curve of solutions for $\alpha \in [0,1]$ whenever the curve is smooth (e.g., [8], [12]). However, the curve of optimum solutions is not necessarily smooth at points corresponding to changes in the set of active constraints. Therefore it is necessary to locate such points and restart the tracing algorithm with a new set of active constraints.

There have been recent attempts to construct algorithms for tracing a path of optimal solutions. Rao and Papalambros [11] use simple continuation to find the family of parametrized optima for large changes in a parameter. Lundberg and Poore [6] use a sophisticated predictor-corrector homotopy curve tracking algorithm to investigate the dependence of the solution on a parameter and to locate bifurcations and points of extreme solution sensitivity. The objective of the present paper is to describe the application of a recently developed homotopy algorithm [9] to tracing optima of bi-objective optimization problems.

[†] Department of Mathematics, Virginia Polytechnic Institute & State University, Blacksburg, Virginia 24061. The work of this author was supported in part by NASA Grant NAG-1-224.

[‡] Department of Aerospace and Ocean Engineering, Virginia Polytechnic Institute & State University, Blacksburg, Virginia 24061. The work of this author was supported in part by NASA Grant NAG-1-224.

[+] Department of Computer Science, Virginia Polytechnic Institute and State University, Blacksburg, Virginia 24061. The work of this author was supported in part by Department of Energy Grant DE-FG05-88ER25068, NASA Grant NAG-1-1079, and Air Force Office of Scientific Research Grant 89-0497.

2. Control-structure optimization. The problem of simultaneous structure-control optimization is formulated as the minimization of the structural weight W and maximum control force $F_{\max}$ subject to constraints on the damping ratios ζ_i of the first n_m vibration modes of the structure.

The equations of motion of the structure controlled by n_c collocated sensors and actuators are written as

$$M\ddot{u} + D_0\dot{u} + Ku = F,$$

where M, D_0 and K are the mass, structural damping and stiffness matrices respectively, u is the displacement vector, F is the applied control force vector, and a dot denotes differentiation with respect to time. A simple direct-rate feedback control law [7] is used for the actuator force vector F given as

$$F = -D_c\dot{u},$$

where D_c is the control matrix which has nonzero rows and columns at positions corresponding to components of $\dot{u}$ measured by the sensors. Assuming that there is no structural damping ($D_0 = 0$), the structure is described by the system

$$M\ddot{u} + D_c\dot{u} + Ku = 0$$

with the general solution $u = u_0 e^{\mu t}$. The stability of the system is controlled by the real parts of the eigenvalues μ_i. The stability margins are characterized by the damping ratios ζ_i defined as

$$\zeta_i = \frac{-\sigma_i}{\sqrt{\sigma_i^2 + \omega_i^2}},$$

where σ_i and ω_i are the real and imaginary parts of μ_i.

We assume that the matrix D_c is positive semidefinite so that the closed loop system has at least the same stability as the open loop system. Following [7] the goal is to have a control system which minimizes the maximum control forces for a given velocity bound $\|\dot{u}\|_\infty \leq U$. The maximum control force applied by the actuators is

$$F_{\max} = \max \frac{\|F\|_\infty}{\|\dot{u}\|_\infty} = \|D_c\|_\infty = \max_i \sum_j |d_{ij}|,$$

where the d_{ij} are the elements of the control matrix D_c.

The problem of simultaneous control-structure optimization is the bi-objective optimization problem

$$\begin{aligned} (1) \qquad & \text{minimize } (W(a), F_{\max}(a, D_c)) \\ & \text{such that } \sum_j |d_{ij}| \leqq F_{\max}, \\ & \zeta_i(a, D_c) \geqq \zeta_{0i} \quad \text{for} \quad i = 1, \ldots, n_m, \\ & D_c \geqq 0, \quad (D_c \text{ positive semidefinite}), \\ & a_i \geqq a_{0i} \quad \text{for} \quad i = 1, \ldots, n_s, \end{aligned}$$

where a is a vector of structural dimensions and $W(a)$ is the structure's weight. The curve of all efficient solutions (designs for which neither $W(a)$ nor $F_{\max}$ can be simultaneously improved) can

be obtained by minimizing the combination $(1-\alpha)W + \alpha F_{\max}$ of the two objective functions for all values of α between 0 and 1. The problem can be rewritten as

$$\text{minimize } c(x,\alpha) = (1-\alpha)W + \alpha F_{\max} \tag{2}$$

$$\text{subject to } G_i(x) = x_{0i} - x_i \leqq 0, \qquad i = 1,\ldots,n_1, \tag{3}$$

$$G_{j+n_1}(x) \leqq 0, \qquad j = 1,\ldots,n_2, \tag{4}$$

where x is the n_1-vector of design variables including a structural size vector a, the nonzero elements of the matrix D_c, and $F_{\max}$. The design variables are subject to the minimum value constraints $x_i \geqq x_{0i}$; the constraints (4) correspond to the other constraints in the problem (1); and α is the parameter assuming all values between 0 and 1. The Lagrangian function and Kuhn-Tucker conditions for this problem are:

$$L(x,\alpha,\lambda) = c(x,\alpha) + \sum_{i=1}^{n_1} \lambda_i (x_{0i} - x_i) + \sum_{j=n_1+1}^{n_1+n_2} \lambda_j G_j(x), \tag{5}$$

$$\frac{\partial c}{\partial x_i} + \sum_{j=n_1+1}^{n_1+n_2} \lambda_j \frac{\partial G_j}{\partial x_i} - \lambda_i = 0, \qquad i = 1,\ldots,n_1, \tag{6}$$

$$G_j \lambda_j = 0, \qquad j = 1,\ldots,n_1+n_2, \tag{7}$$

$$\lambda_j \geqq 0, \qquad j = 1,\ldots,n_1+n_2, \tag{8}$$

$$G_j \leqq 0, \qquad j = 1,\ldots,n_1+n_2. \tag{9}$$

Equations (6)–(7) form a system of nonlinear equations to be solved for the design variables x_i and the Lagrange multipliers λ_j associated with active constraints of the form (4) and with the bounds for design variables (3). The solution (x,α,λ) of these equations, in the generic case, follows a path (not necessarily monotone in α) that consists of several smooth segments, each segment characterized by a different set of active constraints.

3. Homotopy curve tracking. The system of nonlinear equations (6)–(7) is solved by a homotopy curve tracking method. By the Implicit Function Theorem, if $F : E^{N+1} \to E^N$ is C^1, the system of equations

$$F(x,\alpha) = 0 \tag{10}$$

has some solution (x_0,α_0), and the Jacobian matrix $DF(x_0,\alpha_0)$ of the function F at (x_0,α_0) has full rank, then there is some neighbourhood U of (x_0,α_0) such that there is a unique curve of zeros of $F(x,\alpha)$ in U passing through (x_0,α_0). Assuming that 0 is a regular value of F, this full rank of the Jacobian matrix implies that the zero set of (10) contains a smooth curve Γ in $(N+1)$-dimensional (x,α) space, emanating from (x_0,α_0); Γ has no bifurcations and is disjoint from any other zeros of (10). The curve Γ can be parametrized by arc length s:

$$x = x(s), \qquad \alpha = \alpha(s). \tag{11}$$

Taking the derivative of (10) with respect to arc length, the nonlinear system of equations is transformed into the ordinary differential equations

$$[F_x(x(s),\alpha(s)),\quad F_\alpha(x(s),\alpha(s))]\begin{pmatrix}\frac{dx}{ds}\\ \frac{d\alpha}{ds}\end{pmatrix} = 0, \tag{12}$$

and

$$\left\|\begin{pmatrix}\frac{dx}{ds}\\ \frac{d\alpha}{ds}\end{pmatrix}\right\|_2 = 1, \tag{13}$$

where F_x and F_α denote the partial derivatives of F with respect to x and α respectively. With the initial conditions at $s = 0$,

$$x(0) = x_0, \qquad \alpha(0) = \alpha_0, \tag{14}$$

(12)–(14) can be treated as an initial value problem. Its trajectory is the path Γ of optimal solutions $Z(s) = (x(s), \alpha(s))$.

A software package HOMPACK [14], [16], which implements several homotopy curve tracking algorithms, is used to track the zero curve Γ. The HOMPACK algorithms take steps along the zero curve using prediction and correction to find the next point. In the prediction phase a Hermite cubic $p(s)$ is constructed which interpolates the zero curve Γ at two known points, $Z(s_1)$ and $Z(s_2)$. The predicted next point is

$$Z^{(0)} = p(s_2 + h), \tag{15}$$

where $p(s)$ is the Hermite cubic, and h is an estimate of the optimal step (in arc length) to take along Γ.

The corrector iteration is

$$Z^{(k+1)} = Z^{(k)} - \left[DF(Z^{(k)})\right]^+ F(Z^{(k)}), \qquad k = 0, 1, \ldots$$

where $\left[DF(Z^{(k)})\right]^+$ is the Moore-Penrose pseudoinverse of the $N \times (N+1)$ Jacobian matrix DF. In practice this pseudoinverse is not calculated explicitly; see [14] for the details of the Hermite cubic interpolant construction and the corrector iteration.

The parameter α in equations (12)–(14) is a dependent variable, which distinguishes homotopy methods from standard continuation, imbedding, or incremental methods. The homotopy approach is also different from initial value or differentiation methods, since the controlling variable is arc length s, rather than α.

4. Solution along a segment and transition to the next segment. Since the active constraints in a segment are fixed, they can be treated as equality constraints. Furthermore, along each segment some design variables are fixed at their lower bound. The vector of these inactive (passive) variables is denoted x_p and need not be considered as design variables for that segment. The vector of active design variables x_i $(i \in \mathcal{I}_a)$ is denoted as x_a. Along each segment the Kuhn-Tucker conditions are solved for the active design variables x_i $(i \in \mathcal{I}_a)$ and for the Lagrange multipliers λ_g associated with the active constraints of the form (4) $(\lambda_j, j \in \mathcal{I}_g)$. For each segment there are two types of equations:

$$V1 : G_j(x) = 0, \qquad j \in \mathcal{I}_g, \tag{16}$$

$$V2 : \frac{\partial c}{\partial x_i} + \sum_{j \in \mathcal{I}_g} \lambda_j \frac{\partial G_j}{\partial x_i} = 0, \qquad i \in \mathcal{I}_a. \tag{17}$$

The active design variables and the Lagrange multipliers associated with active constraints (4) are the variables in these equations. The homotopy algorithm needs the Jacobian matrix of these functions with respect to α, x_a, and λ_g.

As suggested by the discussion in §3, it is explicitly assumed here that 0 is a regular value of the system defined by (16) and (17), i.e., the Jacobian matrix has full rank along a segment. Let $y = (\alpha, x_a, \lambda_g)$. At the start of a segment the set of active design variables and active constraints for this segment has to be found, so that the vector y is defined. A set of equations is then generated, with the type of each variable determining the form of the equation appended to the system of equations. For a Lagrange multiplier associated with an active constraint of the form (4), the equation has the form (16), and for an active design variable, the equation has the form (17). The system of equations for the segment is solved using the previously described homotopy curve tracking technique. Next the Lagrange multipliers for inactive design variables are calculated according to (6). In these equations the Lagrange multipliers associated with active constraints of the form (4) have been computed by the homotopy method, and the Lagrange multipliers associated with inactive constraints (4) are known to be zero. At each point of a segment the Lagrange multipliers associated with the lower bound of the inactive design variables or the active constraints of the form (4) in the segment should be nonnegative, the value of each G_j, $j = n_1, \ldots, n_1 + n_2$ should be less than or equal to zero, and all design variables should be larger than or equal to their lower bound. If any of the above conditions is not satisfied the segment is terminated and a new one is started. The transition point to a new segment is called here a *switching point.* Depending on the type of termination, the switching point is the point (which is calculated using a guarded secant method, since the curve tracker will have overshot) where

1) one of the positive Lagrange multipliers becomes equal to zero, or
2) a previously negative G_j of the form (4) becomes equal to zero, or
3) an active design variable $x_i (i \in \mathcal{I}_a)$ becomes inactive (equal to x_{0i}).

At the beginning of each segment the system of linear equations (6) is solved for $\lambda_1, \ldots, \lambda_m$, $m = n_1 + n_2$, to check which design variables and constraints are active and to find the initial values of the Lagrange multipliers for the new segment. First the Lagrange multipliers for inactive constraints are set to zero so that Lagrange multipliers only for potentially active constraints (those equal to zero) are considered.

Since some of the constraints (4) may be inactive (their values at the switching point are less than zero), or the derivatives of the constraints (4) with respect to the design variables can assume values for which some columns or rows in the coefficient matrix of the system (6) are linearly

dependent, the rank of this matrix can be less than n_2. The rank of the coefficient matrix for the system (6) determines the number of the constraints (4) which are assumed to be active in the next segment.

The QR factorization with column pivoting is used to find the rank r of the coefficient matrix. (Needing to numerically calculate the rank is a fundamental weakness, closely related to the need to get the active set right in any active set algorithm.) Next the system (6) is solved for all subsets of r columns which are linearly independent assuming that the Lagrange multipliers for the constraints (4) corresponding to the remaining columns are zero. To get the solution for each subset at least r design variables are assumed to be active (the corresponding Lagrange multipliers are set to zero). For each subset of r columns (corresponding to r constraints) all combinations of r out of n_1 design variables are assumed to be active. The system is solved in turn for each combination to find all sets of active design variables and active constraints (4) such that the Lagrange multipliers are nonnegative.

Sometimes there are several solutions satisfying the condition that all the Lagrange multipliers be nonnegative. Then for each solution the signs of the derivatives of the design variables with respect to the arc length s are calculated. To obtain these derivatives it is necessary to compute the derivatives of the design variables with respect to α [3] and multiply them by $\operatorname{sgn}(d\alpha/ds)$ (determined by the direction in which a segment is to be tracked). A set of active constraints (4) and active design variables is accepted when the values of these signs indicate that no active constraint will be immediately violated for increasing values of s. The signs of the derivatives with respect to arc length s are calculated for design variables, Lagrange multipliers and G_j's corresponding to active constraints. A solution is accepted if the derivatives with respect to s of active design variables that are at their lower bound are nonnegative, the derivatives with respect to s of zero Lagrange multipliers that correspond to active constraints (4) are nonnegative and the derivatives of G_j's that are equal to zero are nonpositive.

The path of optimal points can be discontinuous [9], [10]. It is possible that beyond some value of α there are no neighbouring optima. At this point α is fixed and the problem must be solved by a standard optimization algorithm to find a new optimum. Tracking a path of optimal solutions can then be resumed at this new point. It is also possible that beyond a certain value of α no optimum exists, for example, if the problem becomes unbounded. Furthermore, singular points such as bifurcation and fold points may occur [6]. Singular points correspond to a rank deficiency of the Jacobian matrix of the functions given in (16) and (17), which has explicitly been assumed not to occur. Note, however, that since the path parameter is s and not α, a singular F_x is not a problem. It indicates a turning point where $d\alpha/ds$ changes sign. This case has been encountered in the examples discussed in the next section. A more detailed description of this segment switching algorithm is given in Rakowska et al. [9].

Second order optimality conditions [3] are checked to verify that the stationary points found by solving the Kuhn-Tucker conditions are indeed minima. Second order necessary conditions are

$$d^t\left[\nabla^2_{x_a} L\right] d \geqq 0 \quad \text{for every } d \text{ such that } (\nabla G_j)^t d = 0 \quad \forall j \in I_g, \tag{18}$$

where $\left[\nabla^2_{x_a} L\right]_{lm} = \dfrac{\partial^2 L}{\partial x_l \partial x_m}$, $l, m \in \mathcal{I}_a$. When the second order necessary conditions are not satisfied it may still be useful to follow the path of stationary points until the solutions again become optimal. An alternative way of dealing with nonoptimality along Γ is to find a point on another path in the zero set using a standard optimization algorithm.

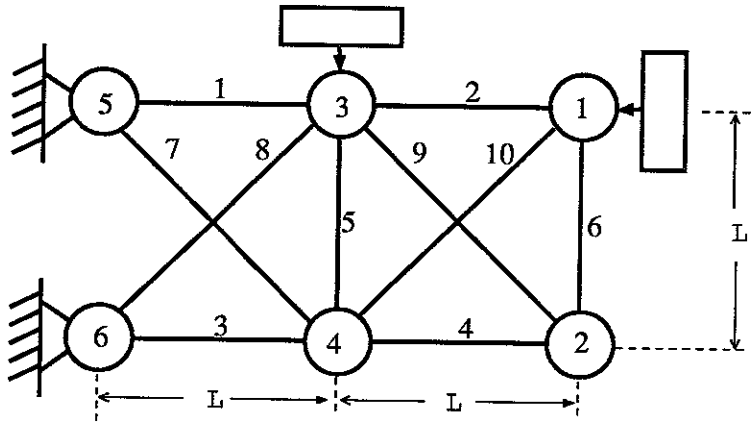

FIGURE 1. *Ten-bar truss with actuators.*

5. Ten-bar truss example. Numerical results are presented here for the ten-bar truss structure shown in Figure 1. Numbers in circles indicate joints and plain numbers label truss elements. The truss is controlled by two pairs of direct-rate feedback collocated sensors and actuators shown by boxes in the figure. The sensors measure velocities, and the actuators apply forces at the positions and directions indicated in Figure 1. The positions of the actuators have been obtained by an optimization that determined the most effective locations for controlling the first four modes. The sensor and actuator pairs are associated with the first (horizontal velocity at joint 1) and sixth (vertical velocity at joint 3) components of the velocity vector $\dot{u}$. The weight of the truss consists of the structural and nonstructural components. The structural weight of the truss is given by $\sum_{i=1}^{10} \rho a_i l_i$, where a_i and l_i are the cross-sectional area and length, respectively, of the i-th truss member and ρ is the weight density. The nonstructural weight is in the form of 4 concentrated masses located at nodes 1, 2, 3 and 4. The first four modes are required to have at least three percent damping ($\zeta_{0i} = 0.03$), $L = 354\,\text{in}$, and the minimum gage area for all truss members is $a_{0i} = 0.1085\,\text{in}^2$. The optimization problem (1) then becomes

$$
\begin{aligned}
\text{minimize } & c(a,\alpha) = (1-\alpha)k\sum_{i=1}^{10} \rho a_i l_i + \alpha F_{\max}, \\
\text{subject to } & G_i = a_{0i} - a_i \leqq 0, \qquad i = 1,\ldots,10, \\
& G_{11} = -d_{11} \leqq 0, \\
& G_{12} = -d_{66} \leqq 0, \\
& G_{13} = -F_{\max} \leqq 0, \\
& G_{14} = |d_{11}| + |d_{16}| - F_{\max} \leqq 0, \\
& G_{15} = |d_{16}| + |d_{66}| - F_{\max} \leqq 0, \\
& G_{j+15} = -0.03 + \zeta_j(a, d_{11}, d_{16}, d_{66}) \leqq 0, \qquad j = 1,\ldots,4, \\
& G_{20} = d_{16}^2 - d_{11}d_{66} \leqq 0,
\end{aligned}
$$

where a is a vector of truss element cross-sectional areas, d_{11}, d_{16}, d_{66} are the nonzero entries of the control matrix D_c, $F_{\max}$ is the control force applied by actuators, and k is a scaling constant taken here to be 0.0261. The design variables in this formulation include the crossectional area vector

TABLE 1
Path of solutions for low nonstructural weight.

Segment	α	$F_{\max}$	W	c	Event
0.	0.00000	2.02826	48.46283	1.26477	$F_{\max}$, d_{11}, d_{16}, d_{66} and G_{15}, G_{16}, G_{20} are active
1.	0.11747	2.02826	48.46283	1.35448	a_1 becomes active
2.	0.18311	1.75177	50.28659	1.39282	Constraint on ζ_2 becomes active
3.	0.37383	1.75176	50.28673	1.47662	a_7 becomes active
4.	0.40406	1.69351	51.70699	1.48846	Constraint on ζ_1 becomes active
5.	0.59911	1.69351	51.70702	1.55557	a_4 becomes active
6.	0.77852	1.67529	53.34251	1.61257	a_6 becomes active
7.	0.89848	1.66523	55.31673	1.64274	a_7 becomes inactive
8.	0.92169	1.66484	55.46817	1.64783	a_3 becomes active
9.	1.00480	1.65938	59.60609	1.65988	α becomes greater than 1

a, the gains d_{11}, d_{16}, d_{66} and $F_{\max}$. The last constraint is the positive semidefinite requirement. Since $F_{\max}$ is not a smooth function of the other design variables, adding it as a design variable removes discontinuities in the derivative of the objective function. Furthermore, the absolute value function $|d_{ij}|$ is not differentiable at zero and so is replaced by a quartic polynomial near zero:

$$|d_{ij}| = \frac{d_t}{2}\left[3\left(\frac{d_{ij}}{d_t}\right)^2 - \left(\frac{d_{ij}}{d_t}\right)^4\right] \qquad \text{for } |d_{ij}| \leqq d_t,$$

where d_t is taken to be 5% of a typical value for d_{ij}.

The results have been obtained for three values of the ratio of the nonstructural weight to structural weight: low (5.51 lb at each of nodes $1,\ldots,4$), medium (22.04 lb at each of nodes $1,\ldots,4$), and high (88.16 lb at each of nodes $1,\ldots,4$). These weights correspond to the ratios 0.4548, 1.8191 and 7.2765 of the nonstructural weight to the weight of the structure when all members are at minimum gage.

The switching points on the path of stationary points for the low weight ratio are shown in Table 1. For $\alpha = 0$ the weight is the only objective, hence the cost function is minimized when all the areas are at minimum gage. The values for d_{11}, d_{16}, d_{66} and $F_{\max}$ were obtained by minimizing the control objective with a standard sequential quadratic programming algorithm (VMCON). The same solution holds for small values of α. For $\alpha \geqq 0.11747$ the derivative of the objective function with respect to a_1 becomes negative and therefore the objective function can be reduced by using a_1 as an active design variable. The homotopy method is used to follow the path of stationary points starting with this value of α.

The path shown in Table 1 consists of 9 segments, with the second column in the table giving α at the beginning of the segment. The last column in the table describes the event that signaled the switching point at the beginning of the segment. Segments are terminated when a design variable or a constraint becomes active, or when an active design variable becomes inactive. Plots of $F_{\max}$

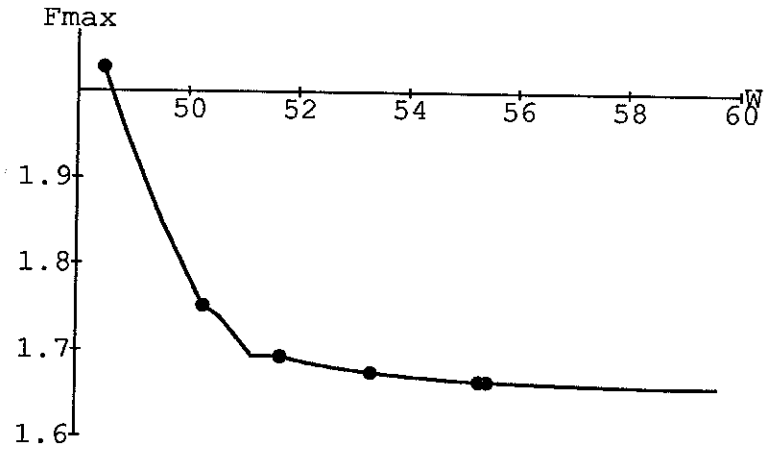

FIGURE 2. *$F_{\max}$ as a function of W for low nonstructural weight.*

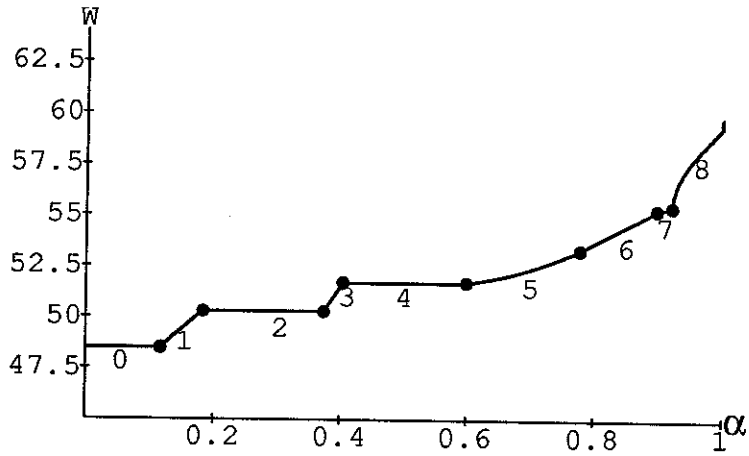

FIGURE 3. *Structural weight W (pounds) for low nonstructural weight.*

as a function of W, the structural weight W as a function of α, and the control force $F_{\max}$ as a function of α, are given in Figures 2, 3, and 4, respectively.

Plots of the weight and the maximum control force indicate that the best designs can be obtained for values of α near 0.4. For these values of α the maximum control force $F_{\max}$ is reduced by 92% of its maximum decrease (corresponding to α changing from 0 to 1), whereas the weight is increased only by 29% of its maximum change. It is interesting to note that along some segments (0, 2, 4) the design is essentially frozen with only the Lagrange multipliers changing.

The path for the medium weight ratio is described in Table 2. Plots of $F_{\max}$ as a function of W and the two components of the objective function W and $F_{\max}$ are given in Figures 5, 6, and 7, respectively. In this case the best designs can be obtained for values of α near 0.8 ($F_{\max}$ reduced by 83% of its maximum change and the weight increased only by 20% of its maximum change).

Along Segments 2 and 4 the design variables again stay essentially at the same value. This time these constant segments account for most of the range of α variation. At the end of Segment 5 no new segment for increasing α can be found. However it is possible to continue the path by

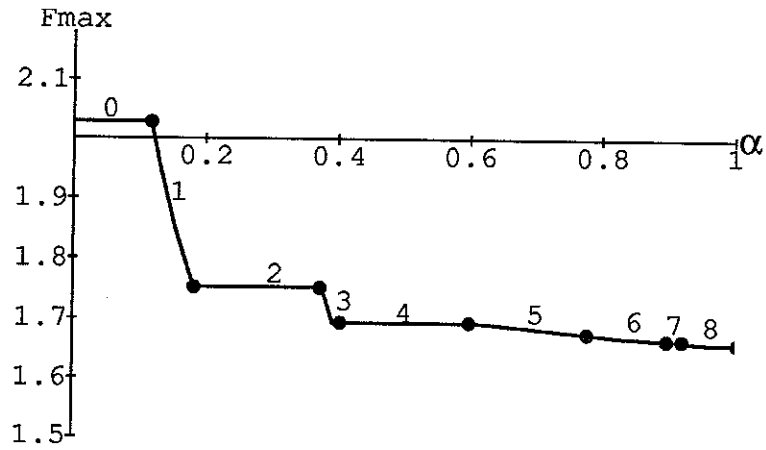

FIGURE 4. $F_{\max}$ *(pounds) for low nonstructural weight.*

TABLE 2
Path of solutions for
medium weight ratio of the nonstructural to the structural weight.

Segment	α	$F_{\max}$	W	c	Event
0.	0.00000	3.02251	48.46283	1.26477	$F_{\max}$, d_{11}, d_{16}, d_{66} and G_{15}, G_{16}, G_{20} are active
1.	0.10921	3.02251	48.46283	1.45844	a_1 becomes active
2.	0.16123	2.74944	50.15051	1.54109	Constraint on ζ_2 becomes active
3.	0.28693	2.74943	50.15056	1.72217	a_7 becomes active
4.	0.31255	2.65683	51.66604	1.75732	Constraint on ζ_1 becomes active
5.	0.83345	2.65683	51.66609	2.43892	a_4 becomes active
6.	0.86770	2.65520	52.02666	2.48356	a_6 becomes active
7.	0.73754	2.60414	58.87609	2.32371	a_7 becomes inactive
8.	0.87005	2.59906	59.62525	2.46354	Constraint on ζ_2 becomes inactive
9.	0.93036	2.54966	76.44878	2.51105	a_5 becomes active
10.	0.94390	2.53224	86.29556	2.51653	a_3 becomes active
11.	0.94940	2.52316	92.48853	2.51763	a_1 becomes inactive
12.	1.00183	2.51446	105.45971	2.51403	α becomes greater than 1

decreasing α to obtain Segment 6. The second order necessary conditions are not satisfied along this segment, so points of Segment 6 are only stationary points for the problem. The path of optimal solutions is resumed in Segment 7. The plot of the objective function in Segments 5, 6, and 7 is magnified in Figure 8. The figure indicates that in the range of $0.738 \leq \alpha \leq 0.870$ there are at least two local minima. Up to about $\alpha = 0.78$, Segment 4 represents the better minimum, and then Segment 7 does.

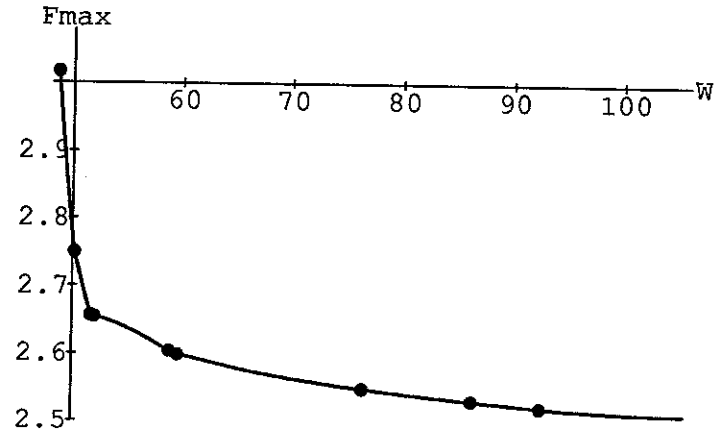

FIGURE 5. $F_{\max}$ *as a function of* W *for medium nonstructural weight.*

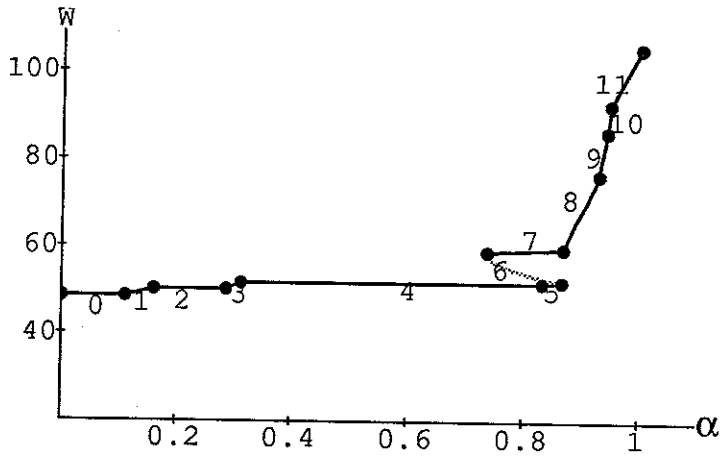

FIGURE 6. *Weight* W *(pounds) for the medium nonstructural weight (gray line denotes nonoptimal stationary points, black line denotes optimal points).*

At points of discontinuity of the path of optimal solutions a standard optimization program (e.g., VMCON) can be used to find a point where the solutions again become optimal. It can be also worthwhile to follow the path of nonoptimal stationary points until a new optimal point is encountered, if the nonoptimal segment is short or if it is difficult to find a point on another optimal branch using standard optimization. In this work the path of stationary points was followed even if they did not satisfy the necessary optimality conditions.

At the beginning of Segment 8 the path of the stationary points can again be tracked only by decreasing the parameter α along a nonoptimal segment. After α decreases from 0.8700583 to 0.8700568 the path of stationary points turns smoothly (F_x becomes singular) and continues for increasing values of α, becoming optimal again. The two components of the objective function, the structural weight W and the control force $F_{\max}$, at the beginning of Segment 8 are shown in Figures 9 and 10, respectively. The scale in Figures 9–10 indicates that the solution undergoes extreme changes in that region with the logarithmic derivative of the weight with respect to α (percent change in W divided by percent change in α) being of the order of 300. This requires tracing the curve with high accuracy.

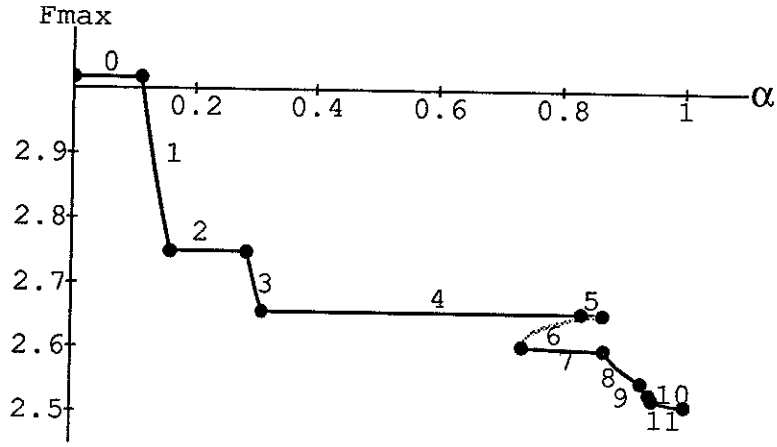

FIGURE 7. $F_{\max}$ *(pounds) for medium nonstructural weight (gray line denotes stationary nonoptimal points, black line denotes optimal points).*

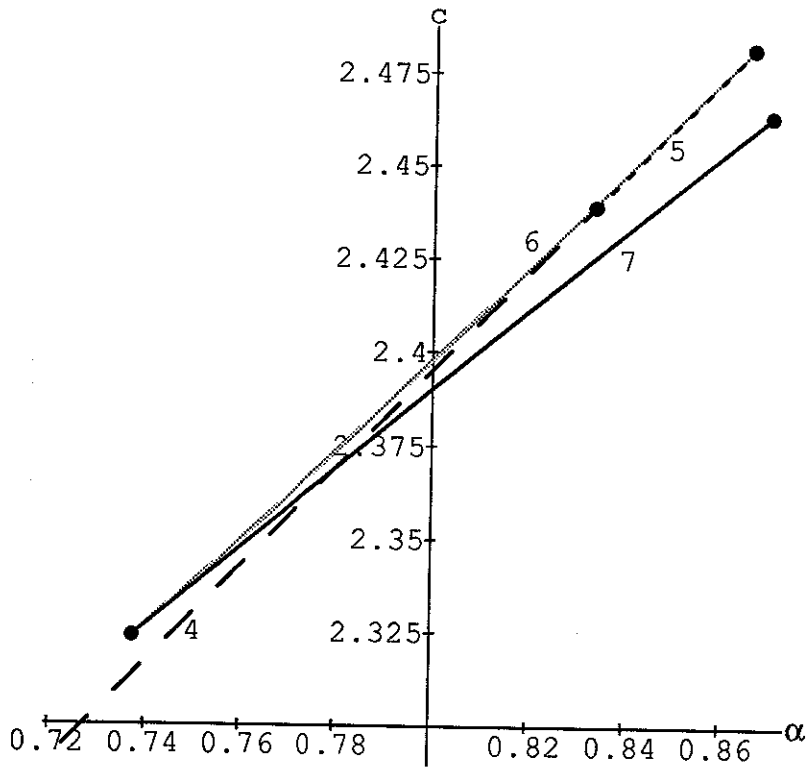

FIGURE 8. *Objective function c (medium nonstructural weight) along Segments 4–7; black lines (4: dashed, 5: dotted, 7: solid) denote optimal solutions, gray line (6) denotes nonoptimal stationary points.*

A similar behavior of the objective function is observed at the beginning of Segment 9. The path of stationary points exists only for decreasing values of α. The path turns smoothly after α decreases by about 0.00013 and continues for increasing values of α. Points corresponding

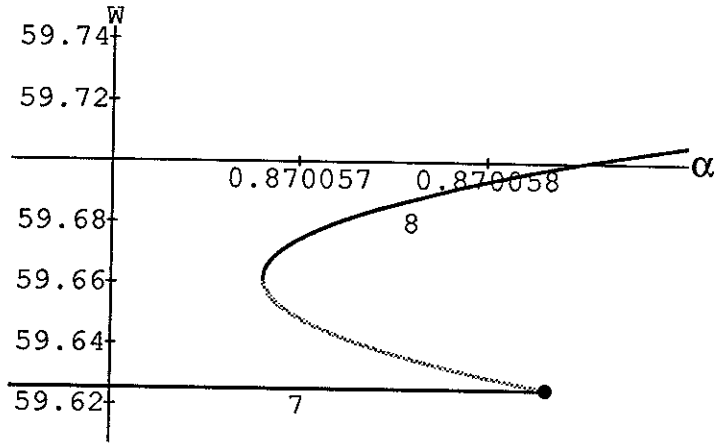

FIGURE 9. *Weight W (medium nonstructural weight) at the beginning of Segment 8 (black line denotes optimal solutions, gray line denotes stationary nonoptimal points).*

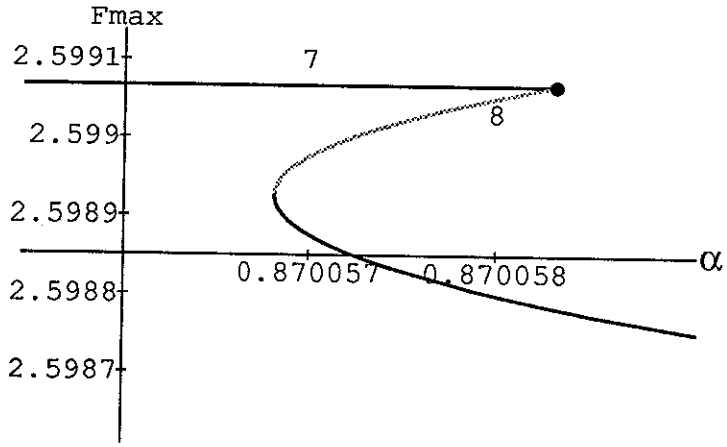

FIGURE 10. $F_{\max}$ *(medium nonstructural weight) at the beginning of Segment 8 (black line denotes optimal solutions, gray line denotes stationary nonoptimal points).*

to decreasing values of α are again nonoptimal points satisfying only the first order necessary conditions.

The path for the high weight ratio is given in Table 3. Plots of the objective function, $F_{\max}$ as a function of W, the control force $F_{\max}$ and the structural weight W are shown in Figures 11, 12, 13, and 14, respectively.

The path consists of three disconnected parts. Part 1 (Segments 0–16) starts at $\alpha = 0$. After α reaches 0.989 at the end of Segment 5, the path continues for decreasing values of α. The optimality conditions are satisfied along the path except for Segment 3 and segments beyond 5. The program was terminated in Segment 16, due to numerical difficulties in calculating damping ratios.

Segment 3 corresponds to decreasing values of α. The plot of the objective function in Segments 2, 3 and 4 (Figure 15) indicates that the end of Segment 2 and the beginning of Segment 4 are only local minima for the problem.

TABLE 3
Path of solutions for high weight ratio of the nonstructural to the structural weight.

Segment	α	$F_{\max}$	W	c	Event
0.	0.00000	5.50241	48.46283	1.26477	$F_{\max}$, d_{11}, d_{16}, d_{66} and G_{15}, G_{16}, G_{20} are active
1.	0.07049	5.50241	48.46283	1.56355	a_1 becomes active
2.	0.11359	4.97967	50.43286	1.73231	Constraint on ζ_2 becomes active
3.	0.29756	4.97967	50.43290	2.40629	a_7 becomes active
4.	0.20892	4.87604	51.54865	2.08296	Constraint on ζ_1 becomes active
5.	0.74981	4.87604	51.54868	3.99269	a_6 becomes active
6.	0.98954	4.87275	52.62111	4.83614	a_{10} becomes active
7.	0.37866	4.76709	57.49997	2.73736	a_4 becomes active
8.	0.26466	4.69717	58.77131	2.37100	Constraint on ζ_1 becomes inactive
9.	0.21374	4.88150	56.56069	2.20399	a_7 becomes inactive
10.	0.17565	4.68689	58.35016	2.07866	Constraint on ζ_2 becomes inactive
11.	0.16091	4.69896	58.26165	2.03194	a_9 becomes active
12.	0.14978	5.12788	55.43446	1.99810	a_4 becomes inactive
13.	0.16106	5.39386	53.70674	2.04461	a_7 becomes active
14.	0.17442	5.32668	54.21070	2.09710	a_6 becomes inactive
15.	0.16120	5.40809	53.58279	2.04474	a_7 becomes inactive
16.	0.12435	5.54933	52.69812	1.89676	a_1 becomes inactive
	0.07236	5.32467	53.42554	1.67872	Program terminated
17.	1.00000	4.54845	211.67533	4.54845	F_{max}, d_{11}, d_{16}, d_{66}, a_3, a_4, a_5, a_6 and G_{15} G_{16}, G_{17}, G_{19}, G_{20} are active
18.	0.99378	4.54915	211.64787	4.55520	Constraint on ζ_3 becomes inactive
19.	0.96882	4.56387	181.89706	4.56959	a_3 becomes inactive
20.	0.95304	4.56442	181.38046	4.57235	a_1 becomes active
21.	0.94695	4.60024	155.98564	4.57216	a_5 becomes inactive
22.	0.88676	4.73885	94.31460	4.48096	Constraint on ζ_3 becomes active
23.	0.79871	4.74453	93.18657	4.27905	a_7 becomes active
	1.00280	4.88803	64.47497	4.89721	α greater than 1, program terminated

Because Part 1 of the curve never reached $\alpha = 1$, we used homotopy with nonstructural weight as the homotopy parameter starting from the point $\alpha = 1$ in the medium nostructural weight case. Part 2 (Segments 17–23) starts therefore at $\alpha = 1$. After α becomes 0.79871 at the end of Segment 22 the path continues for increasing values of α and reaches the point $\alpha = 1$ with larger value of

TABLE 3 (continued)
Path of solutions for high weight ratio
of the nonstructural to the structural weight.

Segment	α	$F_{\max}$	W	c	Event
24.	1.00000	3.81418	90.56545	3.81418	F_{max}, d_{11}, d_{16}, d_{66}, a_3, a_4, a_6, a_9, a_{10} and G_{15}, G_{16}, G_{17}, G_{19}, G_{20} are active
25.	0.94858	3.82382	88.30493	3.74570	Constraint on ζ_3 becomes inactive
26.	0.95335	3.84368	81.18759	3.76323	a_3 becomes inactive
27.	0.92253	3.85193	79.43595	3.71414	Constraint on ζ_1 becomes inactive
	0.19586	4.25997	59.44635	2.08191	Program terminated

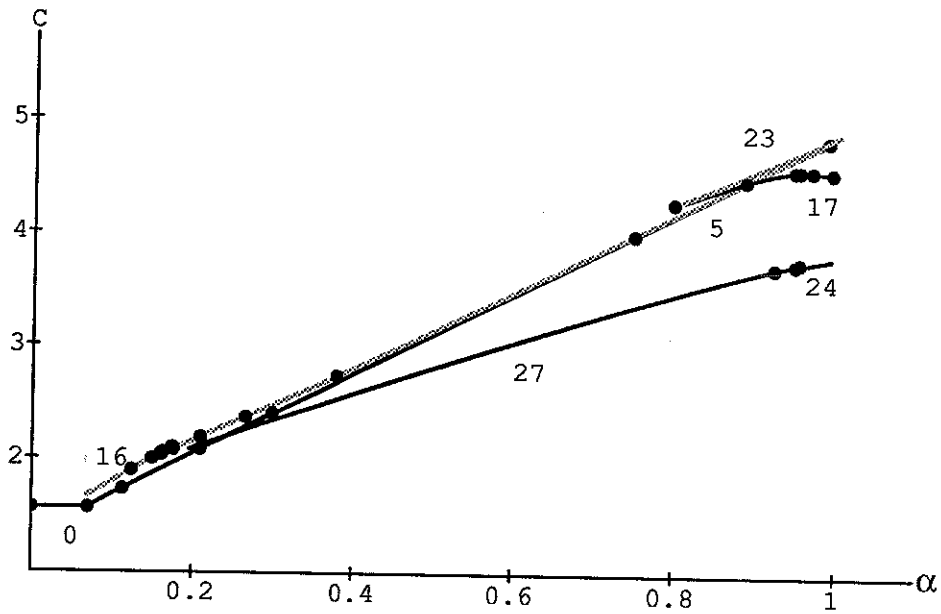

FIGURE 11. *Objective function c for high nonstructural weight.*

the cost function.

The starting point for Segment 24 was found by a standard optimization program MINOS. The cost function along this part of the path is significantly lower than the corresponding values for the two other parts of the path. After α decreases below 0.25 the cost function becomes larger than in part 1 of the path which means that from that point on the path represents only the local minima. The program was terminated at α below 0.2 due to numerical difficulties (problem becomes singular when the eigenvalues μ_i are real). Segment 27 also appears to contain the best compromise design. At $\alpha = 0.39476$, the weight is at 65.04234 which is 39.38% of its total increase while F_{max} is already at 3.93567 which is 92.80% of its total decrease.

6. Concluding remarks. An active set algorithm for tracing parametrized optima was shown to be effective in tracing the efficient curve in bi-objective optimization. The results were

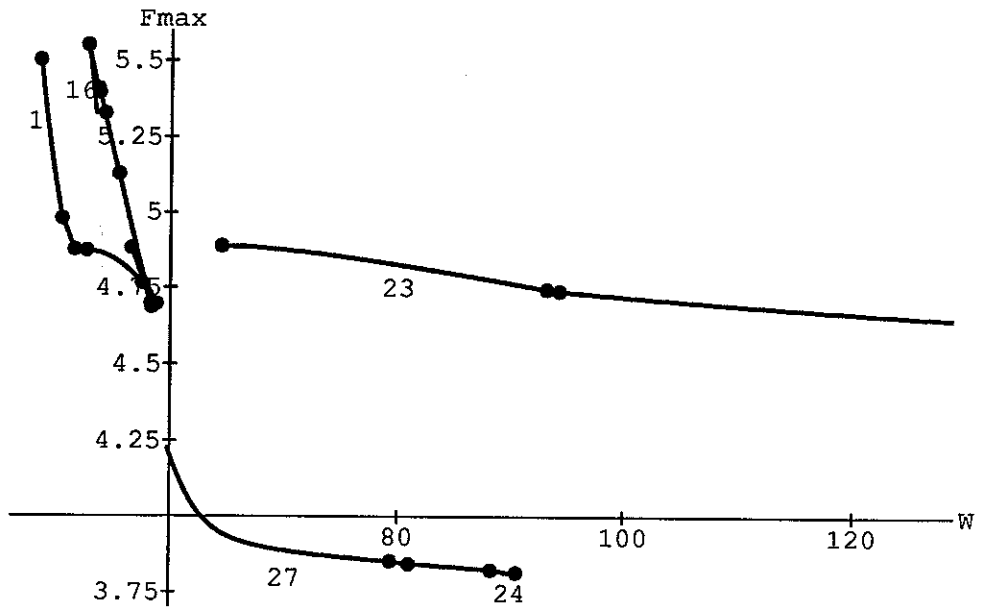

FIGURE 12. $F_{\max}$ *as a function of W for high nonstructural weight.*

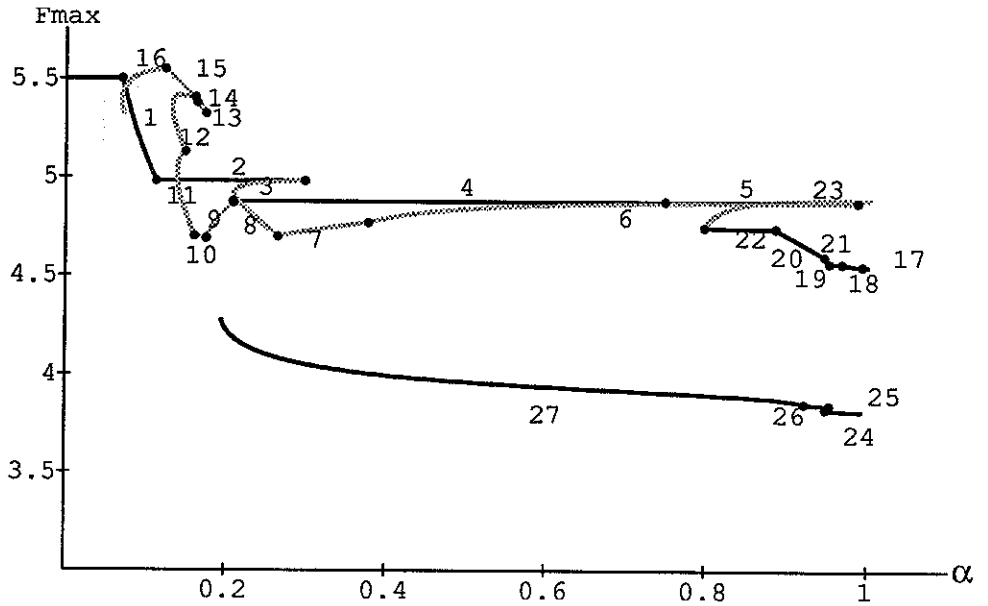

FIGURE 13. $F_{\max}$ *(pounds) for high nonstructural weight (gray line denotes stationary nonoptimal points, black line denotes optimal points).*

obtained for the combined control-structure optimization of a ten-bar truss for three values of the ratio of the nonstructural to the structural weight. On the basis of the efficient curve it was possible to select the value of α which would lead to the best designs. It was found that the efficient curve can be discontinuous and has regions of frozen designs and regions of extremely high variations in the design. Furthermore, in several cases nonoptimal segments of stationary solutions bridged the discontinuities of the efficient curve and thus served as an easy way to continue the tracing process

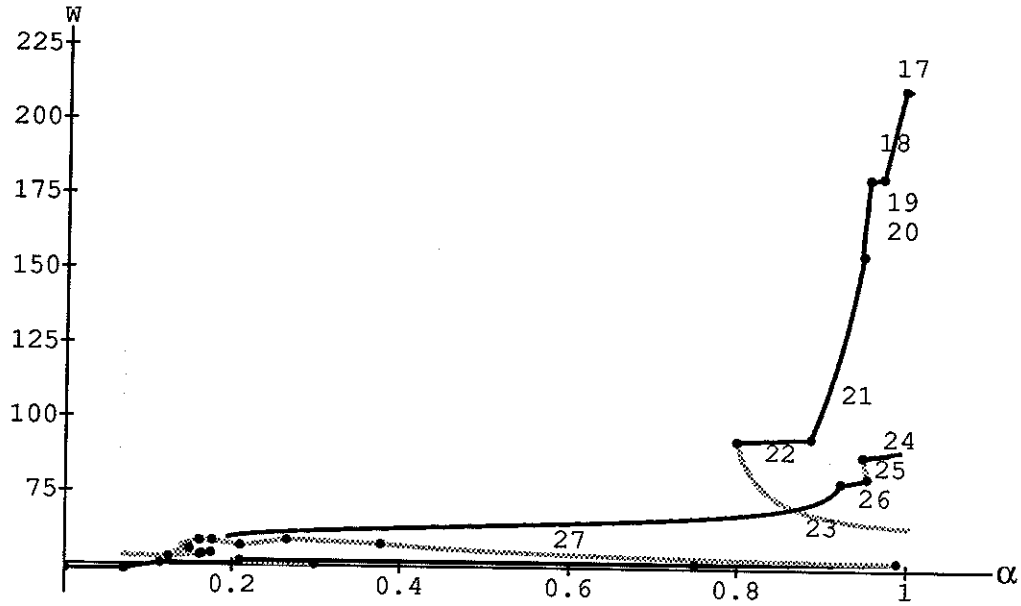

FIGURE 14. *Weight W (pounds) for high nonstructural weight (gray line denotes nonoptimal stationary points, black line denotes optimal points).*

at such discontinuities.

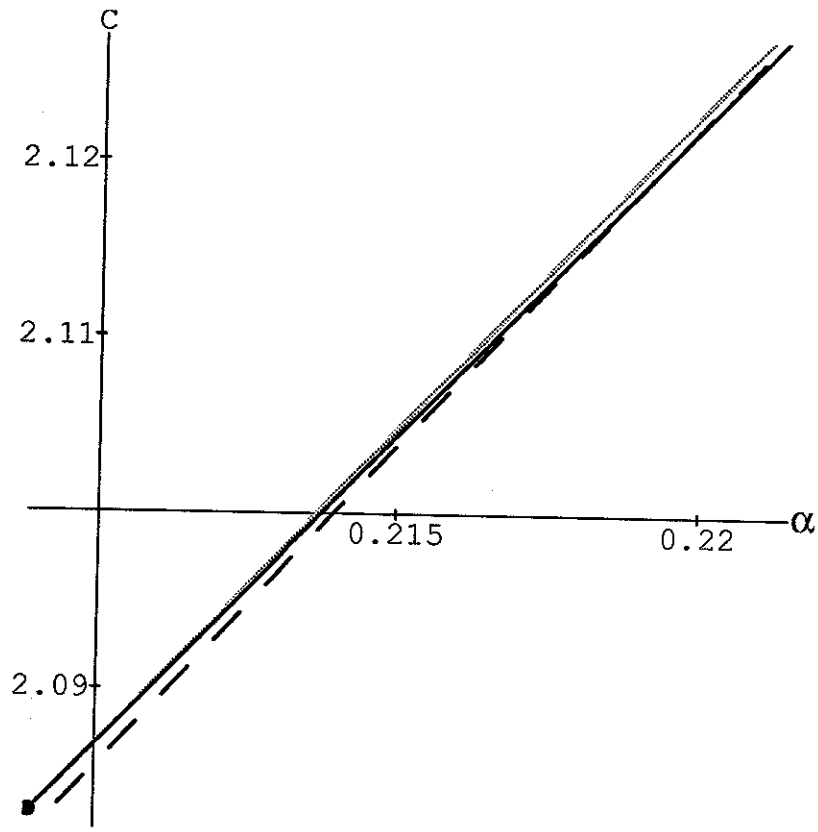

FIGURE 15. *Objective function in Segments 2–4 (2: dashed; 3: gray; 4: solid) for high nonstructural weight.*

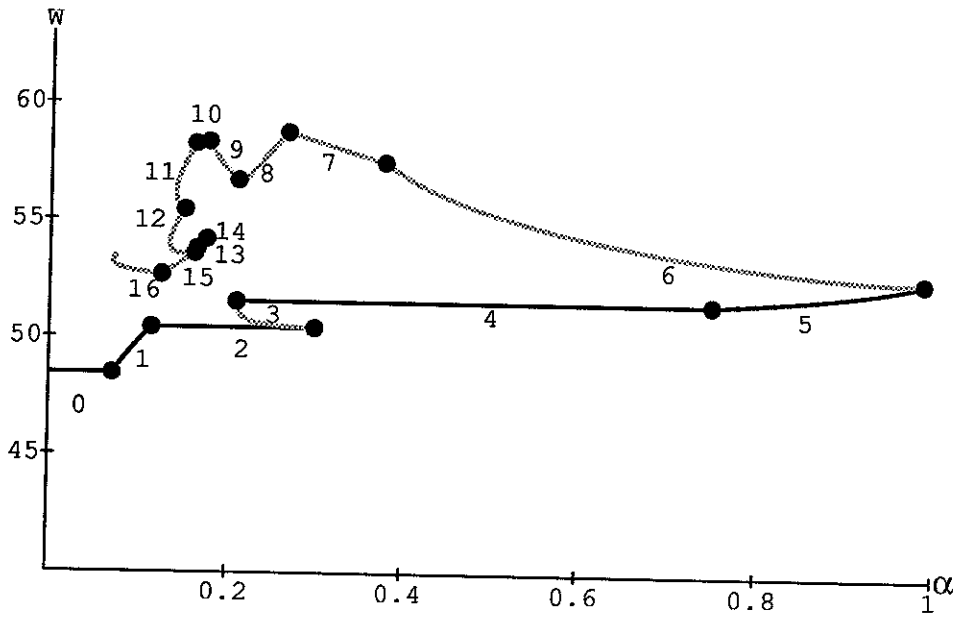

FIGURE 16. *Weight W (pounds), the lower part of the path for high nonstructural weight from Fig.14 (gray line denotes nonoptimal stationary points, black line denotes optimal points).*

REFERENCES

[1] E. L. Allgower and K. Georg, *Introduction to numerical continuation methods*, Springer Verlag, Berlin, Heidelberg, New York, 1990.

[2] H. Eschenaner, J. Koski, A. Osyczka, *Multicriteria design optimization*, Springer-Verlag, New York, 1990.

[3] R. T. Haftka, Z. Gürdal and M. P. Kamat, *Elements of structural optimization*, 2nd ed., Kluwer, Dordrecht, The Netherlands, 1990.

[4] R. T. Haftka, *Integrated structures-controls optimization of space structures*, Proc. AIAA Dynamics Specialist Conference, Long Beach, CA, April 5-6, 1990, pp. 1–9.

[5] K. Lim and J. Junkins, *Robust optimization of structural and controller parameters*, J. Guidance, 12 (1989), pp. 89–96.

[6] B. N. Lundberg and A. B. Poore, *Bifurcations and sensitivity in parametric programming*, Proc. Third Air Force/NASA Symposium on Recent Advances in Multidisciplinary Analysis and Optimization, September 24–26, 1990, San Francisco, CA, pp. 50–55.

[7] Z. N. Martinovic, G. Schamel, R. T. Haftka and W. L. Hallauer, *An analytical and experimental investigation of output feedback vs. linear quadratic regulator*, J. Guidance, 13 (1990), pp. 160–167.

[8] M. Milman, R. E. Scheid, M. Salama and R. Bruno, *Methods for combined control-structure optimization*, Proc. Conference on Dynamics and Control of Large Structures, Blacksburg, VA, May 8–10, 1989, pp. 191–206.

[9] J. Rakowska, R. T. Haftka and L. T. Watson, *An active set algorithm for tracing parametrized optima*, Structural Optimization, to appear.

[10] J. R. J. Rao and P. Y. Papalambros, *Extremal behavior of one parameter families of optimal design models*, Proc. ASME Design Automation Conference, Montreal, Quebec, Canada, Sept. 17–20, 1989, pp. 91–100.

[11] J. R. J. Rao and P. Y. Papalambros, *A nonlinear programming continuation strategy for one parameter design optimization problems*, Proc. ASME Design Automation Conference, Montreal, Quebec, Canada, Sept. 17–20, 1989, pp. 77–89.

[12] M. Salama and J. Garba, *Simultaneous optimization of controlled structures*, Comput. Mech., 3 (1988), pp. 275–282.

[13] H. Wacker, *Continuation Methods*, Academic Press, New York, 1978.

[14] L. T. Watson, *Numerical linear algebra aspects of globally convergent homotopy methods*, Tech. Report TR-85-14, Dept. of Computer Sci., VPI&SU, Blacksburg, VA, 1985, and SIAM Rev., 28 (1986), pp. 529–545.

[15] L. T. Watson, *A globally convergent algorithm for computing fixed points of C^2 maps*, Appl. Math. Comput., 5 (1979), pp. 297–311.

[16] L. T. Watson, S. C. Billups and A. P. Morgan, *HOMPACK: A suite of codes for globally convergent homotopy algorithms*, Tech. Report 85-34, Dept. of Industrial and Operations Eng., Univ. of Michigan, Ann Arbor, MI, 1985, and ACM Trans. Math. Software, 13 (1987), pp. 281–310.